Melting of classical two-dimensional electrons on a helium film: A molecular-dynamics study

Ladir Cândido, José Pedro Rino, and Nelson Studart
Departamento de Física, Universidade Federal de São Carlos, São Carlos, São Paulo, 13565-905, Brazil
(Received 7 March 1996; revised manuscript received 9 May 1996)

Molecular dynamics simulations are employed to study the nature of melting and freezing transitions as well the structural and dynamical properties of the liquid and solid phases of the system formed by classical electrons deposited over a liquid-helium film. The system is very interesting because one can change the form of the pair interaction, from $1/r$ to $1/r^3$, by only varying external parameters. We investigate the influence of the film thickness and different types of substrates on the melting transition by calculating the temperature dependence of the internal energy and the self-diffusion constant. For all substrates considered, we found clear evidence for hysteresis in the temperature dependence of the total energy and self-diffusion, indicating that, as in other charged two-dimensional systems, the system undergoes a first-order transition at a certain value of the plasma parameter Γ defined appropriately to this system. The pair correlation function, the static structure factor, the velocity autocorrelation function, and the frequency spectrum are also evaluated for several film thicknesses and different substrates. [S0163-1829(96)03134-7]

I. INTRODUCTION

The study of charged two-dimensional (2D) systems has attracted considerable interest in the last two decades both for providing a laboratory to test fascinating phase transitions theories and because most of them can be realized experimentally. In particular, electrons on the surface liquid helium have the highest mobilities, because the He surface is smooth and has no impurities, and behave as a nondegenerate electron system.[1] For electrons on the surface of bulk helium, one of the most prominent phenomena is the Wigner classical transition to a solid phase, where the electrons form a triangular lattice.[2] Experimentally, the liquid-to-solid transition takes place for a value of the coupling constant Γ_m (the ratio of potential to kinetic energy) $=137\pm15$. Computer simulations indicate a first-order melting between $\Gamma_c=118$ and 130 with a transition entropy per particle about $0.3k_B$.[3] In contrast to these numerical results, experimental evidence was found that this transition should be continuous in support of the dislocation-pair-unbinding model of Kosterlitz-Thouless.[4]

There have been a number of interesting investigations of the phase transitions for 2D screened charge systems which can be realized experimentally. Two of these are formed by polymer colloids trapped at the water-air interface[5] and colloids confined between two solid surfaces.[6] The interaction between them was found to be a dipole repulsion but a simple Yukawa-like screened Coulomb potential has been also used to describe the quite complicated interaction between the colloids and the medium in which they are immersed. Theoretical studies and computer simulations have been done for both a system of particles interacting with a screened Coulomb[7] and with a 2D dipolar potential.[8]

Electrons in surface states on helium films form also a very interesting system to study the many-body properties of 2D screened systems. In this case the screening is provided by the image charges in the substrate beneath the film. The screening effect can drastically change the interparticle potential. For instance, at low electron densities, when the helium-film thickness is much smaller than the average electron-electron distance and for a metallic substrate, the interaction between electrons is a dipole-dipole interaction. In the opposite limit the usual prototype of a system of electrons on bulk helium is recovered. So the advantage of this system is that the interparticle potential can be varied, *in situ*, by changing the film thickness. The substrate also acts on the electron system by enhancing the stabilizing force and therefore allowing higher densities to be achieved.[9] Therefore quantum effects on the transport properties, quantum melting and possibly the 2D Hall effect can be studied. Peeters and Platzman[10] obtained an approximate phase diagram of electrons on helium films by using a simple dimensional argument and dislocation-mediated melting. One result is a reduction of the melting temperature compared with that in the bulk case. Saitoh[11] obtained a closed-form expression of the melting curve as a function of film thickness and substrate dielectric constant. The static and dynamics properties of the crystal Wigner were investigated by Peeters[12] and subsequent works studied the influence of finite-size effects in the direction normal to the surface in the formation of the 2D Wigner lattice.[13] Collective properties of the electron system both in the classical regime[14] and in the quantum regime have also been determined.[15] Experimentally, Jiang *et al.*[16] reported the phase diagram of electrons on helium films adsorbed over a smooth glass substrate by observing a sharp decrease of the mobility at a certain temperature which was assumed to be the freezing precursor. The investigation of the charge density wave of the classical electron crystal was also reported and it was observed that the crystal is depinned by a sufficiently large electric field applied parallel to the film.[17]

In this paper, we present a study of the behavior and nature of the melting of electrons on helium films by using molecular dynamics (MD) simulations. The MD approach has been shown to have great value in verifying and predicting the structural and dynamical behavior of rather complex systems, in particular the phase and phase transitions in 2D systems.[3,8,18] Beyond the investigation of both equilibrium

and nonequilibrium thermodynamic systems, the MD method provides a powerful tool for studying time-dependent processes. Static quantities like the total energy, pair correlation function, and structure factor as well dynamic properties like the velocity-velocity correlation function, the self-diffusion constant and the vibrational density of modes are determined for several film thicknesses and different substrates. We found the existence of hysteresis and latent heat, indicating that the transition is first order for all substrates considered. We determined the melting temperature for the system for different thicknesses and substrates. In Sec. II, we describe the form of the screened interaction potential and the procedure we have used in the MD simulation. In Sec. III, we present and discuss our results.

II. INTERACTION POTENTIAL AND THE MOLECULAR DYNAMICS PROCEDURE

The interaction pair potential between two electrons above a helium film of thickness d (which we assume to the be same as the distance between the electron layer and the substrate) is given by[19,14]

$$V(r)=2e^2\left[\frac{1}{(1+\epsilon)r}-\frac{2\epsilon}{(1+\epsilon)^2}\sum_{n=1}^{\infty}\frac{\delta^n[(1-\epsilon)/(1+\epsilon)]^{n-1}}{\sqrt{r^2+(2nd)^2}}\right], \tag{1}$$

where $\delta=(\epsilon_s-\epsilon)/(\epsilon_s+\epsilon)$, with ϵ and ϵ_s the dielectric constants of helium and the substrate, respectively. Since the dielectric constant of helium is almost 1 ($\epsilon=1.057$), the series in Eq. (1) converges rapidly and one can retain just the first term and approximate the interaction potential by

$$V(r)=e^{*2}\left[\frac{1}{r}-\frac{\delta}{\sqrt{r^2+(2d)^2}}\right], \tag{2}$$

where $e^*=e/(1+\epsilon)^{1/2}$ is the renormalized electron charge. The screening of the electron-electron interaction due to the substrate appears in the second term of Eq. (2). From Eq. (2) we recover the two opposite limits of the interaction potential. For small interparticle distances ($r\ll d$), the screening is negligible and we obtain the bare potential $V(r)=e^{*2}/r$. On the other hand, if the electrons are far apart ($r\gg d$), the screened interaction has a dipolar term and a Coulomb interaction with an effective electron charge given by

$$V(r)=\frac{(1-\delta)e^{*2}}{r}+\frac{2\delta e^{*2}d^2}{r^3}. \tag{3}$$

Note that for a metallic substrate $\epsilon_s=\infty$, and then $\delta=1$, the interaction is between dipoles of strength $p=2e^*d$ composed of electrons and their image forces.

Our electron system on helium films is embedded in a uniform neutralizing positive background. In order to connect it with one-component plasmas (OCP's), we define a plasma parameter which characterizes the classical OCP for the electron-helium films. This parameter is defined as the ratio of the average potential energy $\langle V\rangle$ to the average kinetic energy $\langle K\rangle$. For the present system with the screened interaction, given by Eq. (2), this becomes

$$\Gamma=\Gamma_c\left[1-\delta\left(1+\frac{4d^2}{a^2}\right)^{-1/2}\right], \tag{4}$$

where $\Gamma_c=e^{*2}/k_BTa$ is the well-known plasma parameter of the OCP with $1/r$ interaction, $a=(\pi n)^{-1/2}$, n is the electron density, and T is the temperature.

The MD simulation was performed for a system of $N=784$ electrons in a rectangular box for a fixed density of 1.477×10^8 cm^{-2} and 1.3×10^{10} cm^{-2} which was the estimated experimental electron density.[16] The sides of the MD rectangle have a ratio of $\sqrt{3}/2$ in such a way that the box is commensurate with the triangular lattice with $4I^2$ (I is an integer) particles in it. The temperature dependence of the total energy for $N=100$ electrons is the same as for larger N; i.e., the internal energy is independent of the size of the system. Periodic boundary conditions were applied and the Ewald method was used to handle the long-range character of the interaction. This leads to an interaction energy given by[12]

$$V(\vec{r})=E_0+U_c\sum_{ij}{\sum_{m_x,m_y}}'\frac{\sqrt{\pi}}{\alpha}\exp(2\pi i\vec{M}\cdot\vec{r_{ij}})L_\delta\left(\frac{\pi^2|\vec{M}|^2}{\alpha^2},\alpha^2\Lambda\right)+\sum_{ij}{\sum_{m_x,m_y}}'\left[\frac{\mathrm{erfc}[\alpha|\vec{r_{ij}}+\vec{\xi}(m_x,m_y)|]}{|\vec{r_{ij}}+\vec{\xi}(m_x,m_y)|}\right.$$
$$\left.-\delta\frac{\mathrm{erfc}[\alpha|\vec{r_{ij}}+\vec{\xi}(m_x,m_y)|^2+\Lambda]^{1/2}}{[|\vec{r_{ij}}+\vec{\xi}(m_x,m_y)|^2+\Lambda]^{1/2}}\right]+N{\sum_{m_x,m_y}}'\left[\frac{\mathrm{erfc}[\alpha|\vec{\xi}(m_x,m_y)|]}{|\vec{\xi}(m_x,m_y)|}-\delta\frac{\mathrm{erfc}[\alpha|\vec{\xi}(m_x,m_y)|^2+\Lambda]^{1/2}}{[|\vec{\xi}(m_x,m_y)|^2+\Lambda]^{1/2}}\right], \tag{5}$$

where

$$E_0=N^2\frac{\sqrt{\pi}}{\alpha}L_\delta(0,\alpha^2\Lambda)-\frac{2N\alpha}{\sqrt{\pi}}+N\delta\sqrt{\Lambda}\,\mathrm{erf}(\alpha\sqrt{\Lambda}),$$

$U_c=e^{*2}/2\sqrt{A}$, with A being the area of the system, $\Lambda=(2d/A)^2$, $\vec{\xi}(m_x,m_y)=m_xf_x\hat{x}+m_yf_y\hat{y}$ is the vector of the real lattice, and $\vec{M}=(m_x/f_x)\hat{x}+(m_y/f_y)\hat{y}$ is the vector of the reciprocal lattice with $f_x=\sqrt{L_x/L_y}$, $f_y=f_x^{-1}$ The function $L_\delta(x,p)$ is defined as

$$L_\delta(x,p)=\int_0^1 x^{-3/2}e^{-z/x}(1-\delta e^{-px}),$$

$\mathrm{erf}(x)$ is the error function, and $\mathrm{erfc}(x)=1-\mathrm{erf}(x)$ is the complementary error function. α is the convergence param-

eter which is used to split the sum into real and reciprocal spaces. The prime in the sums means that the term $m_x = m_y = 0$ or the term $i = j$ is excluded in the summation. The divergent term which appears in the first term of E_0 is canceled out by the contribution coming from the positive and uniform background.

Newton's equations of motion were integrated using a fifth-order predictor-corrector method with time steps of 10^{-12} sec in all calculations which led to a conservation of the total energy of 1 part in 10^4 after several thousands time-step runs. The simulations were performed in cascade; i.e., the equilibrated configuration obtained for a given temperature was used as an input to reach another configuration at higher temperature. A few tests was done in the inverse order, cooling down the system, in order to check the validity of the procedure. The time average of the physical quantities were obtained over 40 000 time steps after the system has been reached the equilibrium. We checked our results for the internal energy and the melting Γ with those obtained for electrons on bulk helium and dipolar systems,[3,8,18] and found them to be in excellent agreement.

III. RESULTS AND DISCUSSION

The solid-liquid transition was studied through the temperature dependence of the total energy per particle and the self-diffusion constant for several film thicknesses and different substrates. Figure 1 displays the total energy per particle versus temperature for a 784-particle system on a helium film supported by a glass substrate ($\epsilon_g = 7.3$, $\delta = 0.75$) (Ref. 16) for three values of film thicknesses $d = 100$, 250, and 350 Å . The electron density is 1.3×10^{10} cm^{-2}. The diamonds and crosses represent the solid and liquid phases, respectively. As one can observe the electron system exhibits hysteresis, supercooling, superheating, and release of latent heat on melting, which is clearly a first-order transition. The vertical dotted lines in Fig. 1 represent the hysteresis region containing the supercooled and superheated phases. The melting entropy is approximately $0.3k_B$, which is the same as that found in other electron systems.[3,8,18] The melting occurs for $106.3 \leqslant \Gamma \leqslant 112.8$ for $d = 100$ Å , $94.0 \leqslant \Gamma \leqslant 87.0$ for $d = 250$ Å , and $92.1 \leqslant \Gamma \leqslant 84.7$ for $d = 350$ Å . It is very clear from Fig. 1 that the melting transition shifts to higher temperatures with increasing the film thickness. This is a consequence of the increase in the screening of the electron gas caused by the substrate (the interaction potential becomes softer) as one decreases the thickness of the film.

In Fig. 2 the temperature dependence of the self-diffusion constant $D = \lim_{t\to\infty} \langle r^2(t)\rangle/4t$, calculated for the system on the solid and liquid lines, is depicted for a film with thickness $d = 100$ Å , electron density 1.477×10^8 cm^{-2}, and two different substrates corresponding to $\delta = 0.08$ and $\delta = 0.75$. The diffusion constant is useful for a criterion for distinguishing a solid from a liquid. In order to investigate in an accurate way the phase transition from a solid to a liquid we have performed additional runs of 100 000 time steps in the metastable region. It should be added that the typical time for homogeneous nucleation of a solid from a liquid in the 2D electron system is about 10 000 MD time steps.[18] We observe that D for this film thickness has two values: zero corresponding to the solid phase and about 0.15 cm^2/sec,

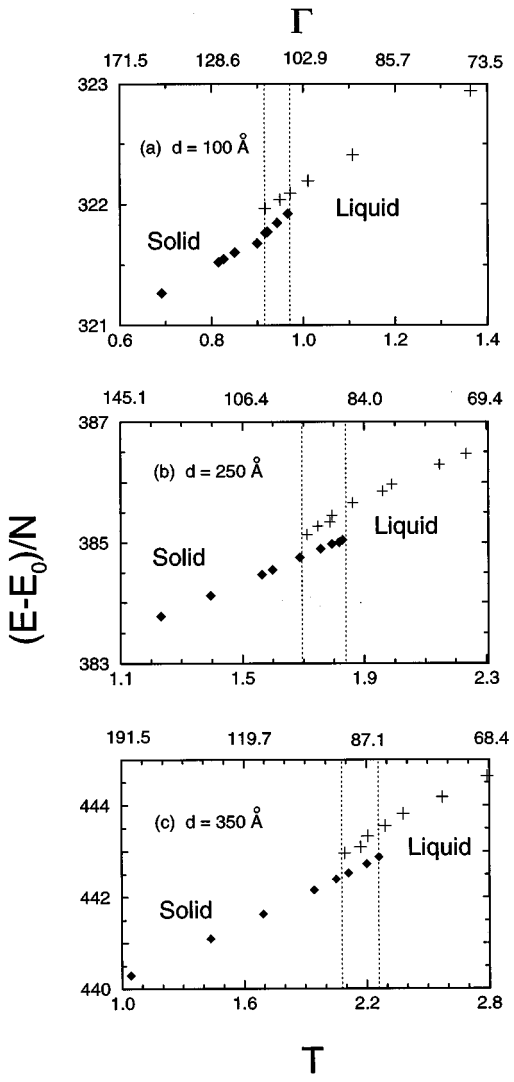

FIG. 1. Variations of the total energy per particle in degrees kelvin (K) with the temperature in units of K and the dimensionless plasma parameter given by Eq. (4) for three film thicknesses. The diamonds and the crosses represent the solid and liquid phases, respectively, and the vertical dotted lines indicate the hysteresis region.

which is four times less than in the case of bulk helium. Note that at this density the melting temperature is considerably smaller than that at higher density as shown in Fig. 2.

The melting temperature versus the film thickness is plotted in Fig. 3 for the glass substrate ($\delta = 0.75$). We also indicate the experimental value T_0 of Jiang, Stan, and Dahm[16] for $d = 240$ Å . We emphasize that $T_0 > T_m$ was assumed to be a melting precursor defined as the intersection of the extrapolation of inverse of the mobility from the fluid and transition regions and there is an uncertainty of 15%–20% in the experimental value of the thickness film. We clearly observe a reduction of the melting temperature as we decrease the film thickness as compared with T_m around 2.8 K which is the upper bound value for the system of electrons on bulk helium.

Figure 4 shows the pair correlation function, which provides information on the structural order, for three film thick-

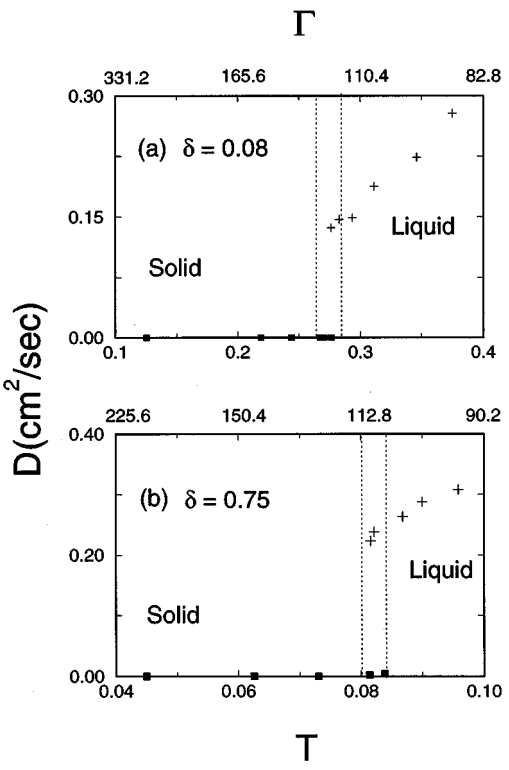

FIG. 2. Self-diffusion constant D vs temperature for a film with $d=100$ Å and different substrates. The results here are for $N=100$ electrons.

nesses. We observe that for a fixed temperature, around $T=1.78$ K, as one increases the film thickness the correlation function exhibits the behavior of a normal liquid ($d=100$ Å) to a supercooled liquid ($d=250$ Å) and finally to a solid ($d=350$ Å), indicated by a shoulder just beyond the second peak, whereas it is smooth in the supercooled liquid. The average coordination number is 6 and the mean distance between electrons is almost constant, indicating an underlying hexagonal structure which is well known in the process of crystallization of 2D systems. In Fig. 5 we analyze the effect of the substrate by showing the pair correlation function for $d=0.02a$, $\Gamma=110$, and different dielectric constants of the

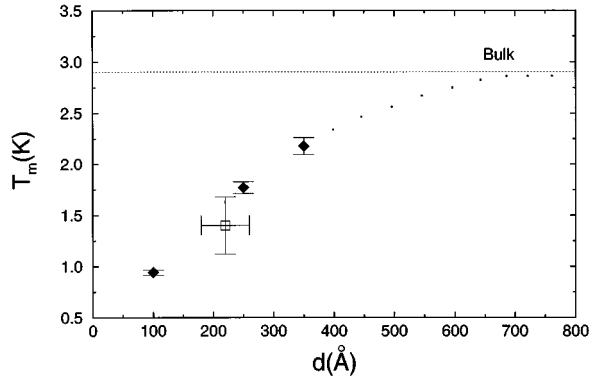

FIG. 3. Melting temperature as a function of the film thickness. The square represents the estimated experimental value given in Ref. 16. The points are guide to the eyes.

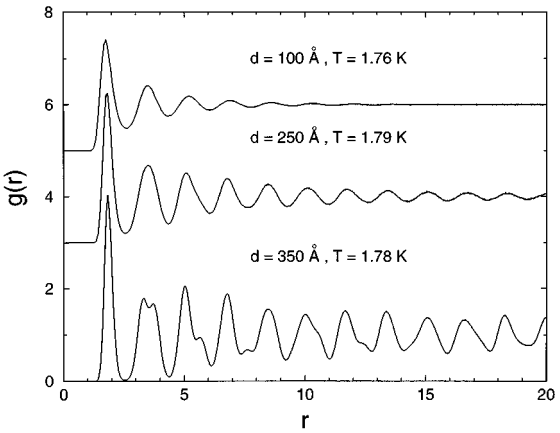

FIG. 4. Pair correlation functions $g(r)$ for a fixed temperature and different thicknesses of a helium film on a glass substrate. The distance is in units of $a=(\pi n)^{-1/2}$. Note the peaks and shoulders in $g(r)$ for the solid system at $d=350$ Å and $T=1.78$ K.

substrate. Note that for this film thickness the system is a normal liquid for $\delta=0.08$ and is a superheated solid for $\delta=0.75$, but behaves like a normal solid in the case of a metallic substrate ($\delta=1.0$). The structure factor $S(q)$, the Fourier transform of $g(r)$, is depicted in Fig. 6 for the same film parameters shown in Fig. 4. Hereafter the properties shown in the figures are calculated for a glass substrate and $N=784$ particle system and density $n=1.3\times10^{10}$ cm^{-2}. As expected the pronounced peak in $S(k)$ for $d=350$ Å occurs very close to the smallest reciprocal vector of the triangular lattice, whereas the peak is quite broad in the normal liquid

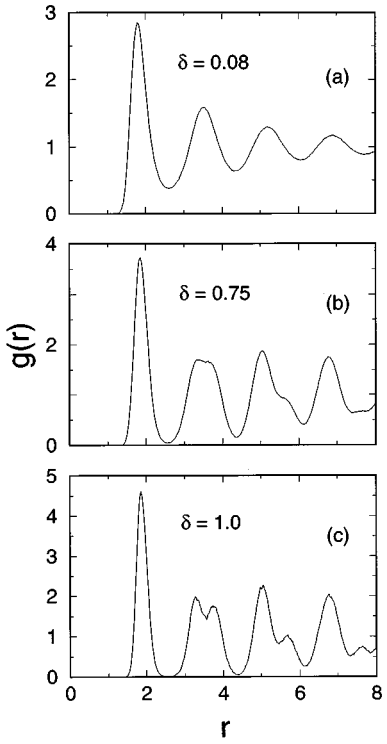

FIG. 5. Pair correlation functions $g(r)$ for $d=0.02a$, $\Gamma=110$, and different dielectric constants of the substrate.

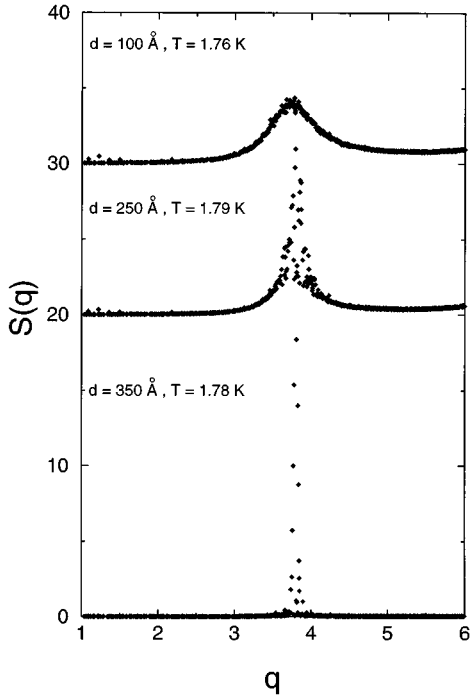

FIG. 6. Structure factors $S(q)$ of the system for a fixed temperature and different thicknesses of a helium film on a glass substrate. The wave vector is in units of a^{-1}.

($d=100$ Å) due to thermal effects. The overall behavior of the structure factor is the same for different substrates.

We also find evidence of the liquid and the solid phases in the dynamic properties of the system. The normalized velocity autocorrelation function $Z(t)=\langle v(t)v(0)\rangle/\langle v(0)\rangle^2$is depicted in Fig. 7. The function $Z(t)$ exhibits a series of oscillations with a frequency 1.2 τ^{-1}, where τ is the temperature-independent unit of time given by $\tau=(ma^2/\langle V\rangle)^{1/2}$. The upper curve is for a liquid above melting, and the middle curve is for a supercooled liquid in the hysteresis region, whereas the lower curve is for a normal solid. We also checked that the period of oscillation is almost independent of the size of the system by performing simulations with

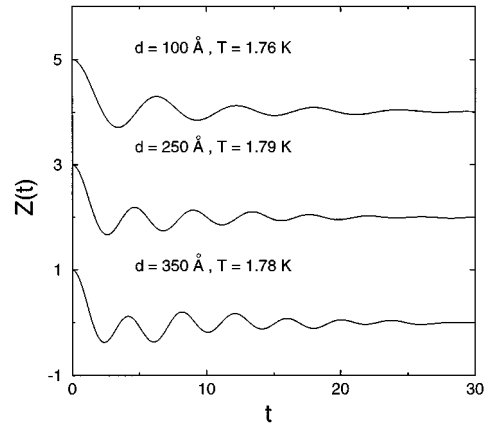

FIG. 7. Time dependence of normalized velocity autocorrelation functions $Z(t)$ for a fixed temperature and different thicknesses of a helium film on a glass substrate. The time scale is in picoseconds.

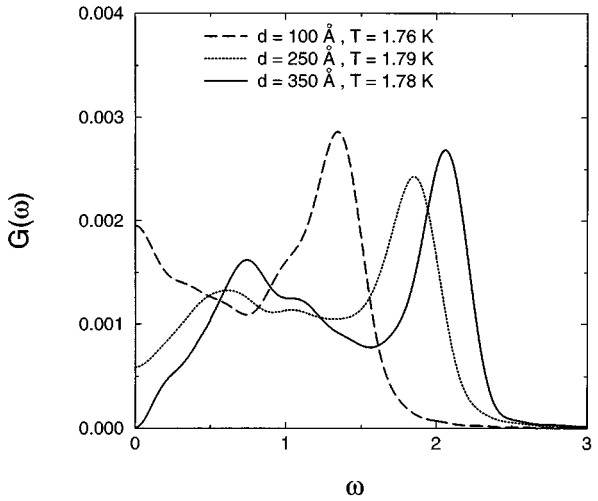

FIG. 8. Frequency spectrum $G(\omega)$ for the same parameters of previous figures. The frequency is in units of the plasma frequency $\omega_p=(2\pi ne^2q/m)^{1/2}$, where q is taken as the smallest wave vector in the MD box.

different particle numbers. In Fig. 8 we show the Fourier transform of the velocity autocorrelation function $G(\omega)$ which is the frequency spectrum of the system for a fixed temperature and three film thicknesses. It is important to point out that $G(0)$is proportional to the diffusion constant D, and it is clear from the figure that for $d=350$ Å , the zero-frequency value of $G(\omega)$ vanishes, as expected. The frequency spectrum for $d=350$ Å at $T=1.78$ K has two peaks reminiscent of a solid hexagonal structure[12,20] and as one decreases the film thickness the first peak disappears and only the peak corresponding to the diffusive motion survives. As one decreases the film thickness at this temperature the system is found to be in the liquid phase since $G(0)$ is nonzero.

In conclusion, we investigated the nature of the melting transition for the system of electrons confined over the surface of liquid helium which in turn is deposited on a solid substrate. On the basis of the MD results, we conclude that the melting of the system is a first-order transition, as other 2D charged classical systems. We described the correlational and dynamical properties of the systems by varying the external parameters of the system like the film thickness and the dielectric constant of the substrate. We are able to reproduce previous results to the pure electron system with a $1/r$ interaction like the dipolar system. We found a reduction of the melting temperatures as one decreases the film thickness. These results should be useful to the experimental investigation of the melting transition in this system.

ACKNOWLEDGMENTS

This work was partially sponsored by Conselho Nacional de Desenvolvimento Científico e Tecnológico (CNPq) and Fundação de Amparo à Pesquisa do Estado de São Paulo (FAPESP). One of us (L.C.) is supported by Fundação Coordenação de Aperfeiçoamento de Pessoal de Nível Superior (CAPES).

[1] For reviews, see C. C. Grimes, Surf. Sci. **73**, 379 (1978); F. I. B. Williams, *ibid.* **113**, 371 (1982); Yu. P. Monarkha and V. B. Shikin, Fiz. Nizk. Temp. **8**, 563 (1982) [Sov. J. Low Temp. Phys. **8**, 279 (1982)]; N. Studart and O. Hipólito, Rev. Bras. Fis. **16**, 194 (1986); P. Leiderer, J. Low Temp. Phys. **87**, 247 (1992).

[2] C. C. Grimes and G. Adams, Phys. Rev. Lett. **42**, 795 (1979); K. Shirahama and K. Kono, **74**, 781 (1995).

[3] R. K. Kalia, P. Vashishta, and S. W. de Leeuw, Phys. Rev. B **23**, 2794 (1981).

[4] F. Gallet, G. Deville, and F. I. B. Williams, Phys. Rev. Lett. **49**, 588 (1982); G. Deville, A. Valdes, E. Y. Andrei, and F. I. B. Williams, *ibid.* **53**, 588 (1984); D. C. Glattli, E. Y. Andrei and F. I. B. Williams, *ibid.* **60**, 420 (1988); D. C. Glattli, G. Deville, V. Duburck, F. I. B. Williams, E. Paris, B. Etienne, and E. Y. Andrei, Surf. Sci. **229**, 344 (1990).

[5] P. Pieranski, Phys. Rev. Lett. **45**, 569 (1980).

[6] P. Pieranski, L. Strzlecki, and B. Pansu, Phys. Rev. Lett. **50**, 900 (1983); C. A. Murray and D. M. van Winkle, *ibid.* **58**, 1200 (1987); C. A. Murray and R. A. Wenk, *ibid.* **62**, 1643 (1989); R. E. Kusner, J. A. Maan, J. Kerins, and A. J. Dahm, *ibid.* **73**, 3113 (1994).

[7] H. Cheng, P. Dutta, D. E. Ellis, and R. Kalia, J. Chem. Phys. **85**, 2332 (1986); F. M. Peeters and X. Wu, Phys. Rev. A **35**, 3109 (1987).

[8] R. K. Kalia and P. Vashishta, J. Phys. C **14**, L643 (1981); V. M. Bedanov, G. V. Gadiyak, and Yu. E. Lozovok, Phys. Lett. **92A**, 400 (1982).

[9] H. Etz, W. Gombert, and W. Idstein, Phys. Rev. Lett. **53**, 2567 (1984); H. Ikezi and P. M. Platzman, Phys. Rev. B **23**, 1145 (1981); V. V. Tatarskii, Fiz. Nizk. Temp. **12**, 451 (1986) [Sov. J. Low Temp. Phys. **12**, 255 (1986)]; X. L. Hu and A. J. Dahm, Phys. Rev. B **42**, 2010 (1990).

[10] F. M. Peeters and P. M. Platzman, Phys. Rev. Lett. **50**, 2021 (1983).

[11] M. Saitoh, Phys. Rev. B **40**, 810 (1989).

[12] F. M. Peeters, Phys. Rev. B **30**, 159 (1984).

[13] M. Šunjic' and Z. Lenac, Europhys. Lett. **11**, 431 (1990); Z. Lenac and M. Šunjic', Phys. Rev. B **43**, 6049 (1991); **44**, 11 465 (1991).

[14] Yu. P. Monarkha, Fiz. Nizk. Temp. **3**, 1459 (1977) [Sov. J. Low Temp. Phys. **3**, 702 (1977)]; J. P. Rino, N. Studart, and O. Hipólito, Phys. Rev. B **29**, 2584 (1984).

[15] U. de Freitas, L. C. Iorriati, and N. Studart, J. Phys. C **20**, 5983 (1987).

[16] H.-W. Jiang, M. A. Stan, and A. J. Dahm, Surf. Sci. **196**, 1 (1988).

[17] H.-W. Jiang and A. J. Dahm, Phys. Rev. Lett. **62**, 1396 (1989); Surf. Sci. **229**, 352 (1990).

[18] P. Vashishta and R. K. Kalia, in *Melting, Localization and Chaos*, edited by R. K. Kalia and P. Vashishta (North-Holland, Amsterdam, 1982), p. 43; F. F. Abraham, *ibid.* p. 75; K. J. Naidoo, J. Schnitker, and J. D. Weeks, Mol. Phys. **80**, 1 (1993).

[19] W. R. Smythe, *Static and Dynamic Electricity* (McGraw-Hill, New York, 1950), p. 192.

[20] L. Bonsall and A. A. Maradudin, Phys. Rev. B **15**, 1959 (1977).